The dynamic properties of zircon studied by single-crystal X-ray diffraction and Raman spectroscopy

Article *in* European Journal of Mineralogy · September 2001

DOI: 10.1127/0935-1221/2001/0013-0939

3 authors:

Boris Kolesov
Russian Academy of Sciences
149 PUBLICATIONS **2,497** CITATIONS

SEE PROFILE

Charles A. Geiger
University of Salzburg
245 PUBLICATIONS **4,311** CITATIONS

SEE PROFILE

Thomas Armbruster
University of Milan
177 PUBLICATIONS **3,379** CITATIONS

SEE PROFILE

Eur. J. Mineral.
2001, **13**, 939-948

The dynamic properties of zircon studied by single-crystal X-ray diffraction and Raman spectroscopy

BORIS A. KOLESOV[1)], CHARLES A. GEIGER[2)]* and THOMAS ARMBRUSTER[3)]

[1)] Institute of Inorganic Chemistry, Lavrentiev prosp. 3, Novosibirsk 630090, Russia
[2)] Institut für Geowissenschaften, Universität Kiel, Olshausenstr. 40, D-24098 Kiel, Germany
[3)] Laboratorium für chemische und mineralogische Kristallographie,
Universität Bern, Freiestrasse 3, CH-3012 Bern, Switzerland

Abstract: An investigation of the dynamic properties of synthetic non-metamict zircon, $ZrSiO_4$, was undertaken using X-ray single-crystal diffraction and polarized single-crystal Raman spectroscopy. The X-ray results at room temperature show that the Zr cation located on the triangular dodecahedral site is tightly bonded. The atomic displacement parameters from different crystals and refinements on zircon are compared and shown to be different. This is probably a result of experimental problems associated with extinction and/or slight degrees of metamictization in natural samples. A calculation of the librational motions of the rigid SiO_4 tetrahedron give a mean-square libration of 3.3(3) degree^2 along the *a* axes and 6.9(6) degree^2 along the *c* axis. The Raman spectrum shows some unusual features, such as the low wave number SiO_4 bending motion, υ_2, at 266 cm^{-1}, that can be explained by the structural properties of zircon. The structure is characterized by open 'channels' running parallel to [001] and they influence the energies of the SiO_4 bending modes depending upon their symmetries. The Raman modes differ strongly in intensity and this can be explained by vibrational interactions with the electronic state of Zr^{4+}. In contrast to garnet, which shares a few structural similarities with zircon, the Zr cation residing in the large dodecahedral site shows little dynamic disorder. In addition, all the external modes in zircon are harmonic in comparison to a few modes in pyrope garnet, for example, that soften with decreasing temperature.

Key-words: zircon, X-ray diffraction, lattice dynamics, Raman spectroscopy.

Introduction

Zircon, $ZrSiO_4$, is found in many different geologic environments (Speer, 1980). Probably its most important application is in U-Pb age dating, because U readily substitutes for Zr in the structure. Recent interest in zircon has centered around its potential use as a host phase for the disposal of radioactive actinides such as weapons plutonium (Ewing *et al.*, 1995). Natural zircon is typically characterized by varying degrees of metamictization that results from the radioactive decay of U and Th. This leads to structural changes characterized by a loss of translational symmetry. The structure of synthetic non-metamict and various natural metamict zircons has been studied by X-ray and neutron diffraction methods a number of times (*e.g.*, Hassel, 1926; Krstanovic, 1958; Robinson *et al.*, 1971; Finger, 1973; Hazen & Finger, 1979; Siggel & Jansen, 1990; Mursic *et al.*, 1992a, b; Rios *et al.*, 2000). The static crystal structure at ambient conditions and its behavior under pressure and at elevated temperatures are well described. Vibrational spectra, including single-crystal polarized Raman and IR measurements, have also been made on natural and synthetic zircon and the optic phonons at the zone center have been carefully measured (Dawson *et al.,* 1971; Syme *et al.*,

*E-mail: chg@min.uni-kiel.de

DOI: 10.1127/0935-1221/2001/0013-0939 0935-1221/01/0013-0939 $ 2.50

1977). There have also been a number of studies using Raman spectroscopy to characterize the degree and nature of metamictization in zircon (Zhang *et al.*, 2000 and references therein).

Nevertheless, with regard to end-member non-metamict zircon several aspects of the crystal structure and lattice dynamics have not been addressed and additional study is useful. One point of interest regards the behavior of the Zr^{4+} cation in the large triangular dodecahedral site. This site in zircon is similar to the triangular dodecahedral site in garnet (Robinson *et al.*, 1971). Single-crystal X-ray work on silicate garnets has shown that the divalent **E**-site cations on this site are anisotropically and dynamically disordered (Armbruster & Geiger, 1993) and this was confirmed in other measurements, for example, by the vibrational spectra of pyrope, $Mg_3Al_2Si_3O_{12}$, (Kolesov & Geiger, 1998; Geiger *et al.*, 1992). The dynamic behavior of Zr^{4+} in zircon has not been directly investigated. In addition, its vibrational spectrum shows interesting and unusual features that have not yet been explained. For example, a B_{1g} Zr-SiO_4 translational mode is characterized by a high wave number of 393 cm^{-1}, whereas an internal SiO_4 bending mode (υ_2) occurs at 266 cm^{-1}. The Raman modes also show large differences in intensity and the reason(s) for this are not completely clear.

We have undertaken a combined single-crystal

Table 1. X-ray data collection and refinement parameters.

Crystal size (mm)	0.15 x 0.05 x 0.05
Diffractometer	Enraf Nonius CAD4
X-ray radiation	sealed tube Mo$K\alpha$, graphite monochromatized
X-ray power	55 kV, 40 mA
Temperature	293 K
Reflections measured	3672
max. θ (°)	56
Unique reflections > 4σ(I)	394
space group	$I4_1/amd$ (No. 141) origin at center
cell dimensions (Å)	a = 6.6039(6), c = 5.9783(4)
R(int) after empirical absorption correction	2.2 %
R(σ)	2.7 %
Number of l.s. parameters	12
GooF	1.077
R1, $F_o > 4\sigma(F_o)$	1.54 %
wR2 (on F^2)	3.89 %

Note: F_o: observed structure factor, F_c: calculated structure factor

$$R(int) = \Sigma \left| F_o^2 - F_o^2(mean) \right| / (F_o^2)$$

$$R(\sigma) = \Sigma \left[\sigma(F_o^2) \right] / \Sigma(F_o^2)$$

$$R1 = \left(\Sigma \| F_o| - |F_c| \| \right) / \left(\Sigma |F_o| \right)$$

$$wR2 = \sqrt{\left(\Sigma \left(w \left(F_o^2 - F_c^2 \right)^2 \right) / \left(\Sigma w \left(F_o^2 \right)^2 \right) \right)}$$

$$GooF = \sqrt{\left(\Sigma \left(w \left(F_o^2 - F_c^2 \right)^2 \right) / (n - p) \right)}$$

n: number of F, p: number of l.s. parameters

$$w = 1/[\sigma^2(F_o^2) + (0.0187P)^2 + 1.0P] \text{ , where } P = [\text{ Max } (F_o^2, 0) + 2F_c^2] / 3$$

X-ray diffraction and polarized Raman spectroscopic study of a well characterized and structurally 'perfect' synthetic zircon, having no metamictization, to address these issues.

Experimental methods and theoretical background

Crystals

Zircon crystals grown by the flux method by Chase & Osmer (1966) were kindly provided by G.R. Rossman. They are optically clear, ranging from about 1 mm to several mm in size, and can be described as having gem quality. The {100} crystal faces, as well as {111} terminating pyramids, are well developed. Optical examination of the crystals with a binocular and microscope revealed no inclusions or zoning. The very narrow line widths of the Raman bands indicate a highly crystalline structure without major zoning or defects.

X-ray experimental

A small fragment, *ca.* $0.15 \times 0.05 \times 0.05$ mm^3 in size, was separated from a large crystal and studied with a single-crystal X-ray diffractometer at room temperature (293 K). Cell dimensions were refined from the angular settings of 14 reflections with $45 < 2\theta < 60°$ yielding tetragonal symmetry. Experimental details are given in Table 1. Intensity data in the half sphere of reciprocal space between $25 < \theta < 56°$ were collected. Low-angle data were omitted, because test measurements revealed severe extinction problems (Finger, 1973). Data reduction, including background and Lorentz polarization correction, was carried out with the SDP program system (Enraf Nonius, 1983). An empirical absorption correction using the ψ-scan technique was applied. Systematic absences confirmed the space group $I4_1/amd$. Structure solution and refinement were performed with neutral-atom scattering factors and the programs SHELXS-97 and SHELXL-97 (Sheldrick, 1997). All atoms were refined with anisotropic displacement parameters. The high crystal quality, leading to a very low mosaic spread, required an empirical extinction parameter to be refined.

Raman experimental

Polarized Raman spectra were recorded with a Triplemate, SPEX spectrometer with a CCD detector, LN-1340PB, from Princeton Instruments. The 514 nm line of an Ar laser was used for spectral excitation. The spectra were obtained in back-scattering geometry. The laser beam was focused to a diameter of 2 μm using a LD-EPIPLAN, 40/0.60 Pol., Zeiss objective. The spectral slit was 2 cm^{-1}. The spectra were collected for about 5 minutes. The laser output power was about 300 mW and the power on the crystal was about 10 mW. Because of the high transparency of the crystal, there was no significant heating.

Results and discussion

X-ray diffraction

The atomic coordinates for the Zr, Si and O atoms from the X-ray refinement are given in Table 2. They agree well with previous determinations. Our coordinates are in excellent agreement with those of Siggel & Jansen (1990), but are slightly more precise. Small differences exist between the various structure refinements of 'undamaged' zircon which could be a result of minor metamictization in the natural samples and/or problems related to extinction (Robinson *et al.*, 1971; Finger, 1973; Hazen & Finger, 1979; Siggel & Jansen, 1990).

The structure of zircon can be described as consisting of chains of alternating edge-sharing SiO_4 tetrahedra and ZrO_8 triangular dodecahedra running parallel to the *c* axis (Robinson *et al.*, 1971). Similar dodecahedral-tetrahedral chains occur in garnet, but in three directions. The chains are linked to one another laterally by edge-sharing between dodecahedra. There are two crystallographically independent Zr-O bonds (4x) of lengths 2.1279(4)

Table 2. Atomic coordinates and isotropic displacement parameters.

Atom	x	y	z	B_{eq}
Zr	0	3/4	1/8	0.303(2)
Si	0	3/4	5/8	0.319(3)
O	0	0.06586(7)	0.19533(7)	0.518(4)

Table 3. Anisotropic displacement parameters in the form of U_{ij} recalculated from single-crystal X-ray studies of weakly metamict or synthetic zircon.

Reference	atom	U_{11}	U_{22}	U_{33}	U_{23}
Robinson *et al.* (1971)	Zr	0.0021(2)	0.0021(2)	0.0022(2)	
Finger (1973)	Zr	0.0056(2)	0.0056(2)	0.0042(4)	
Hazen & Finger (1979)	Zr	0.0038(2)	0.0038(2)	0.0029(2)	
Siggel & Jansen (1990)	Zr	0.0031(1)	0.0031(1)	0.0027(2)	
This study	Zr	0.00364(6)	0.00364(6)	0.00427(7)	
Robinson *et al.* (1971)	Si	0.0031(3)	0.0031(3)	0.0049(5)	
Finger (1973)	Si	0.0072(2)	0.0072(2)	0.0046(11)	
Hazen & Finger (1979)	Si	0.0038(2)	0.0038(2)	0.0029(2)	
Siggel & Jansen (1990)	Si	0.0031(2)	0.0031(2)	0.0022(5)	
This study	Si	0.00402(8)	0.00402(8)	0.0041(1)	
Robinson *et al.* (1971)	O	0.0082(8)	0.0069(7)	0.0052(7)	0.0000(8)
Finger (1973	O	0.0121(13)	0.0072(13)	0.0081(13)	0.0011(13)
Hazen & Finger (1979)	O	0.0106(8)	0.0049(8)	0.0036(8)	-0.0012(8)
Siggel & Jansen (1990)	O	0.0087(3)	0.0042(3)	0.0039(3)	-0.0007(2)
This study	O	0.0093(1)	0.0045(1)	0.0058(1)	-0.0008(1)

Note: e.s.d's of U_{ij} for the structures given by Robinson *et al.* (1971), Finger (1973), and Hazen & Finger (1979) were estimated from their data.

Å and 2.2684(4) Å. The Si-O bond length (4x) is 1.6225(4) Å. The atomic displacement parameters (Table 3) show that the Zr^{4+} cation is tightly bonded and that its vibrational behavior is not strongly anisotropic. In fact, the B_{eq} displacement parameter for Zr is slightly smaller than that of Si (Table 2). The anisotropic U_{ij} values for Si are identical and, therefore, the Si cation shows no directionalized vibrational behavior. The U values for Zr are a little different from those of Si (*i.e.*, U_{11} and U_{22} are a little bit smaller and U_{33} is the same).

In addition to the structural data provided herein, there are four other single-crystal X-ray studies on pure end-member or slightly metamict zircon at ambient conditions (Robinson *et al.*, 1971; Finger, 1973; Hazen & Finger, 1979; Siggel & Jansen, 1990). It should be noted, however, that none of the previous studies aimed for a precise determination of the atomic displacement parameters (adp's). Experience has shown that random and systematic experimental errors strongly influence their quality. In addition, in natural zircon U^{4+} and Hf^{4+} substitution and the degree of metamictization must be considered (even if the authors regard their zircon as non-metamict). In synthetic samples the low degree of mosaic domains gives rise to severe extinction problems associated with multiple diffraction phenomena, both of which are difficult to correct for. In order to compare the adp's of the different studies, we have transformed the displacement parameters from the different published zircon structures to U_{ij} values (Table 3). From the data of Robinson *et al.* (1971) only their B_{eq} value for oxygen could be reproduced from the β_{ij} values, but not B_{eq} for Zr and Si from their β_{ij} values. Hazen & Finger (1979) give the same β_{ij} values and associated estimated standard deviation (esd's) for both Zr and Si in their work, which is unlikely, because displacement parameters of Zr (40 electrons) can be determined with a higher accuracy than those of Si (14 electrons). A comparison of the U_{ij} values calculated from the different refinements shows that individual U_{ij} values for Zr and Si are different by up to a factor of two. Surprisingly, there is better agreement for the lighter oxygen. These discrepancies are probably caused by the experimental difficulties mentioned above.

In order to better understand the displacement parameters, we calculated the differences between the anisotropic mean-square displacements evaluated along internuclear directions ($\Delta U = U(O) - U(Me)$). ΔU values tend to be less affected by systematic errors than absolute U values, because systematic errors in U tend to cancel one another when taking the difference (*e.g.*, Kunz & Armbruster, 1990). In addition, studies have shown (Kunz & Armbruster, 1990; Armbruster & Geiger, 1993 and references therein) that the values along a Si-O vector [*i.e.*, $\Delta U = U(O) - U(Si)$] are typically 0.0004 $Å^2$ providing an additional check on data quality. Table 4 gives the esd's of the difference displacement parameters from the dif-

Table 4. ΔU's evaluated along the bonding vector $\Delta U = U(O) - U(Me)$.

Reference	Si-O	Zr-O (2.27Å)	Zr-O (2.13Å)	e.s.d
Robinson *et al.* (1971)	0.00224	0.00357	0.00461	>0.001
Finger (1973)	0.00257	0.00495	0.00241	>0.001
Hazen & Finger (1979)	-0.00023	0.00191	0.00050	>0.001
Siggel & Jansen (1990)	0.00066	0.00181	0.00083	0.0004
This study	0.00026	0.00215	0.00050	0.0002

Note: e.s.d's of U_{ij} for the structures described in Robinson *et al.* (1971), Finger (1973), and Hazen & Finger (1979) were estimated from their data.

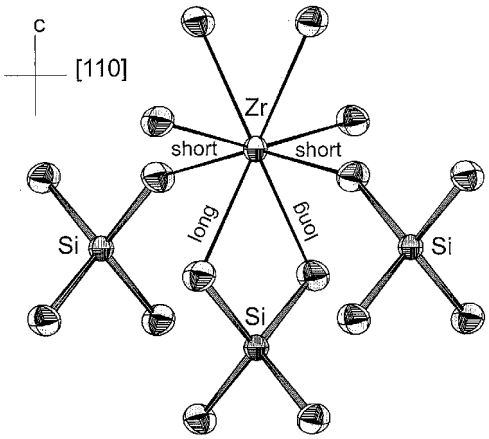

Fig. 1. Fragment of the zircon structure showing the ZrO_8 triangular dodecahedron formed by the four shorter (*ca.* 2.13 Å) and four longer (*ca.* 2.27 Å) Zr-O bonds and SiO_4 tetrahedra. Oxygen probability ellipsoids can be described by librational motions of rigid SiO_4 tetrahedra around the *a* and *c* axes.

ferent studies (Robinson *et al.*, 1971; Finger, 1973; Hazen & Finger, 1979). They are so large that little information can be obtained from the calculated ΔU values (*e.g.*, the esd's are about three times larger than the expected value along the Si-O vector). The data of Siggel & Jansen (1990) and of this study agree within 1 esd with the assumed ΔU value along the Si-O vector. In addition, there is also good agreement within 1 esd for the two different Zr-O vectors. It can be concluded that oxygen vibrates more strongly parallel to the longer Zr-O bond of *ca.* 2.27 Å, thus increasing ΔU, compared to its behavior parallel to the shorter Zr-O bond of *ca.* 2.13 Å. A librational motion of the rigid SiO_4 tetrahedron parallel to the *a* axes has a stronger effect on the oxygen associated with the longer Zr-O bond (Fig. 1). Its libration, following Schomaker & Trueblood (1968), yields a mean-square libration of 3.3(3) degree^2 about the *a* axes and 6.9(6) degree^2 about the *c* axis. The mean-square translational motion of the SiO_4 tetrahedron is isotropic with 0.0041(1) Å^2 along the *a* axes and 0.0043(1) Å^2 along the *c* axis.

In contrast, if calculations for the SiO_4 groups are performed using refinement data of a radiation-damaged zircon (Rios *et al.*, 2000), the mean-square librational disorder about the *a* axes is 5.6(8) degree^2 and 5.6(1.6) degree^2 about the *c* axis. The mean-square translational disorder of the SiO_4 tetrahedron becomes anisotropic with 0.0067(2) Å^2 along the *a* axes and 0.0043(3) Å^2 along the *c* axis. These data confirm the suggestion by Rios *et al.* (2000) that the zircon structure is softer along the *a* axes, thus allowing for increased displacements in radiation damaged crystals. Their comparison of the isotropic displacement parameters for an undamaged zircon (Robinson *et al.,* 1971) versus those of a radiation-damaged zircon (Rios *et al.*, 2000) suggested that radiation damage appears to effect Zr and O more than Si. This statement has to be revised if our zircon data are considered. It appears that radiation damage has a similar effect on all three atoms Zr, Si, and O.

Raman spectra

In zircon there are four formula units in the *I*-centered cell or two in a primitive cell. The Zr and Si atoms occupy the 4a and 4b crystallographic positions respectively, both with site symmetry $\bar{4}m2 = D_{2d}$ (V_d). The oxygen atoms occupy 16h positions with $m = C_s$ (C_{1h}) symmetry. Group theory and symmetry analysis provide the number of normal modes and their symmetry (Dawson *et al.*, 1971; Syme *et al.*, 1977). From this, the total irreducible representation at the Γ–point can be given as follows:

$$\Gamma = 2A_{1g} + A_{2g} + 4B_{1g} + B_{2g} + 5E_g + A_{1u} + 3A_{2u} + B_{1u} + 2B_{2u} + 4E_u.$$

Table 5. Symmetry analysis of $ZrSiO_4$. T - translations, R - restricted rotations. The upper half gives a normal mode analysis and the bottom half gives the wave numbers and assignments of the observed Raman (this work) and IR modes (from Dawson *et al*., 1971).

	A_{1g}	A_{2g}	B_{1g}	B_{2g}	E_g	A_{1u}	A_{2u}	B_{1u}	B_{2u}	E_u
Zr			1(*c*)		1(*a,b*)		}1(*c*)			}1(*a,b*)
$T(SiO_4)$			1(*c*)		1(*a,b*)					
$R(SiO_4)$		1(*c*)			1(*a,b*)			1(*c*)		1(*a,b*)
$(OSiO)_{bend}$, ν_2	1			1		1	1		1	
$(OSiO)_{bend}$, ν_4			1		1					1
$(SiO)_{str}$, ν_1	1						1		1	
$(SiO)_{str}$, ν_3			1		1					1
			215		202		338			287
Observed			393		225					
modes					356					389
(cm^{-1})	439			266			608			
			641		546					430
	974						989			
			1008		923					885

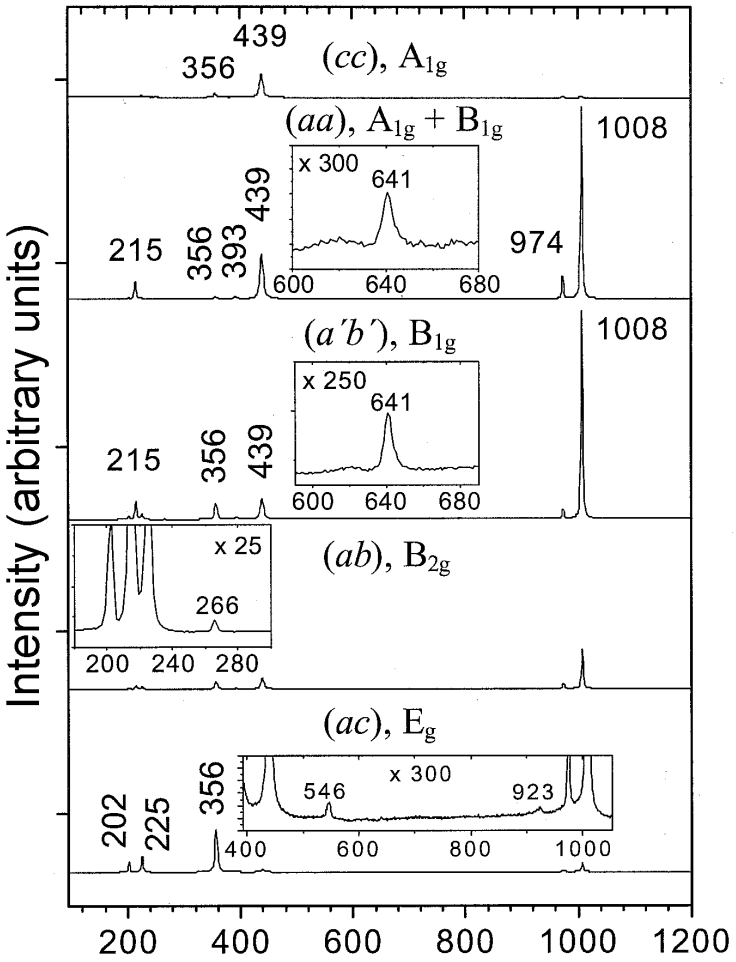

Fig. 2. Polarized Raman spectra of zircon. The first letter defines the polarization direction of the incident radiation and the second letter that of the scattered radiation. The prime symbols denote a coordinate system rotated 45° around the *c* axis.

The A_{1g}, B_{1g}, B_{2g} and E_g modes are Raman active, for a total of 12, and the A_{2u} and E_u modes are active in the infrared. Table 5 gives the modes and their symmetry.

The polarized Raman spectra of zircon are shown in Fig. 2. The bottom part of Table 5 lists the wave numbers of the observed Raman and infrared active modes. The latter are taken from Dawson *et al.* (1971). The spectra and wave numbers of our Raman modes are in excellent agreement with other studies (*e.g.*, Dawson *et al.*, 1971; Syme *et al.*, 1977). The general lattice dynamical properties of zircon are discussed well in both of these reports. The spectra contain, however, some features that have not been addressed and, therefore, warrant further discussion. First, there is a large difference in intensity between the different modes. For example, the A_{1g} mode at 974 cm^{-1} is moderately intense in the (*aa*) spectrum, but its intensity is negligible in (*cc*). This is difficult to understand considering the point symmetry of the SiO_4 tetrahedron. The intensities of the SiO_4 υ_4-bending modes, which typically lie in the wave number region of 500-700 cm^{-1} (Kieffer, 1985), are very weak, as is the υ_2 bending mode at 266 cm^{-1} in the B_{2g} spectrum. This was observed before (Syme *et al.*, 1977) and, in fact, this υ_2 mode was not detected in some measurements (*e.g.*, Nicola & Rutt, 1974) The A_{1g} υ_2 mode at 439 cm^{-1} is, in contrast, strong. In addition, their wave numbers are considerably different.

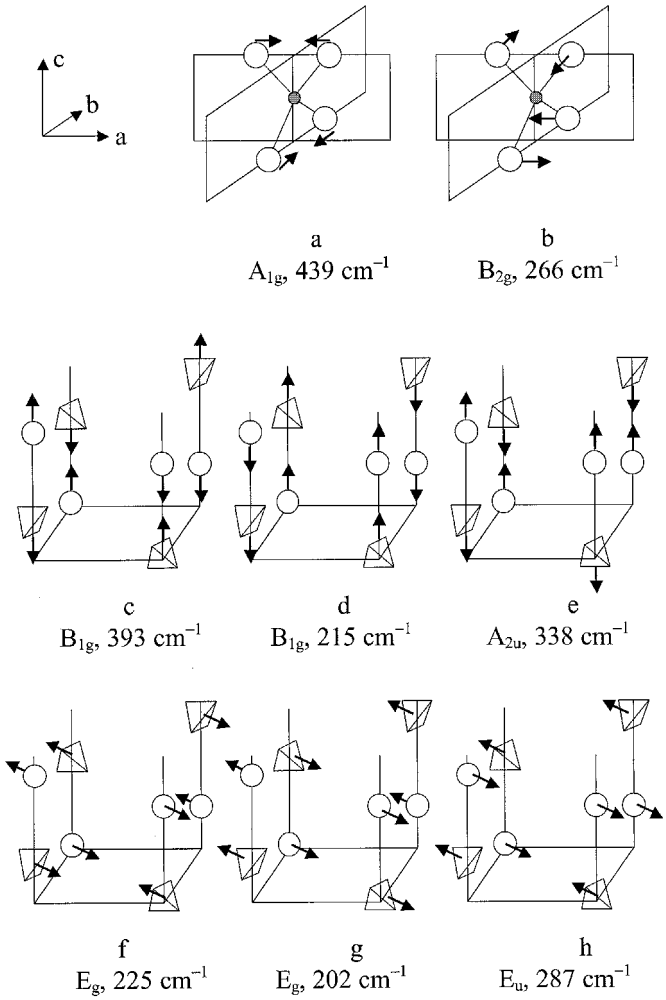

Fig. 3a-h. Schematic depiction of the low wave number vibrational modes in zircon.

To address these issues, we should first consider the assignment of the modes. The vibrations in zircon can be divided into internal SiO_4 modes and external modes of the Zr cation and SiO_4 groups vibrating against one another (Dawson *et al.*, 1971; Syme *et al.*, 1977). In general, the internal SiO_4 stretching vibrations will occur at the highest energies and the external vibrations at the lowest energies. These studies showed that the force constants of the cation-oxygen bonds are considerably different. The Si-O bond has a value of 9.01 m dyn Å^{-1} and the two Zr-O bonds have values of 0.94 m dyn Å^{-1} and 0.96 m dyn Å^{-1}. Thus the mode at 974 cm^{-1} of A_{1g} symmetry can be assigned to a υ_1 internal symmetric stretching of the SiO_4 tetrahedron. The other four high-energy modes at 1008 cm^{-1} (B_{1g}), 923 cm^{-1} (E_g), 989 cm^{-1} (A_{2u}) and 885 cm^{-1} (E_u) are assigned to υ_3 asymmetric stretching motions. It is known that for the internal SiO_4 bending modes, υ_2 and υ_4, the latter occurs at higher wave numbers. This is because the Si atom takes part in υ_4 and not in υ_2 (*i.e.*, the participation of Si decreases the reduced mass of the vibrating system and, hence, increases its energy). The two weak bands in the Raman spectra at 641 cm^{-1} (B_{1g}) and 546 cm^{-1} (E_g) and the two bands in the IR at 608 cm^{-1} (A_{2u}) and 430 cm^{-1} (E_u) can therefore be assigned to υ_4 modes. Two υ_2 modes are only active in the Raman and we assign them to the bands at 439 cm^{-1} (A_{1g}) and 266 cm^{-1} (B_{2g}). The latter has an energy that is lower than some external modes (see below). This is not the case in other orthosilicates (*e.g.*, garnet, olivine). The intensity of the B_{2g} mode is much weaker than that of the A_{1g} mode.

The zircon structure can be described as having two planes parallel to (010) and (100) that contain all the atoms and their bonds. Structurally, the planes define open 'channels' that run parallel to [001]. It may be expected, therefore, that the vibrational behavior will be different for vibrations occurring within these planes compared to those perpendicular to them. The A_{1g} and B_{2g} SiO_4 bending modes are components of a twofold degenerate υ_2 vibration that is split in the crystal field. They are depicted in Fig. 3a and b. For the A_{1g} mode at 439 cm^{-1}, the oxygen atoms vibrate within either the (010) or (100) plane and modulate the nearest neighbor Zr-O and O···O bonds. This is not the case for the B_{2g} mode at 266 cm^{-1}, where the oxygen atoms vibrate perpendicular to (010) and (100) and towards the open channels. We believe this can explain the difference in wave number and intensity between the two υ_2 modes. It also indicates the important role of Zr.

For the lower-energy external modes, one E_g (356 cm^{-1}) and one E_u (389 cm^{-1}) vibration are assigned to librations of the SiO_4 groups (or mixed rotation-translations). This that agrees with the assignment of Symes *et al.* (1977) but not of Dawson *et al.* (1971), the latter of whom assigned the 356 cm^{-1} mode to a υ_4 bending vibration. There are five E_g modes in total and the energy of a SiO_4 libration should lie between those of the internal SiO_4 vibrations and the translational modes. Silicate garnets have a R(SiO_4) mode with a similar energy (Kolesov & Geiger, 1998). Finally, the B_{1g} modes at 215 and 393 cm^{-1}, the E_g modes at 202 and 225 cm^{-1}, the A_{2u} mode at 338 cm^{-1}, and the E_u mode at 287 cm^{-1} are assigned to Zr-(SiO_4) translations. The lowest energy mode at 202 cm^{-1} and the highest at 393 cm^{-1} differ by nearly a factor of two. This is unexpected, because the mass of Zr and SiO_4, 91.22 and 92.08 atomic mass units (a.m.u.), respectively, are similar. For the B_{1g} and A_{2u} modes translational motion occurs along the *c* axis, where the Zr^{4+}-Si^{4+} distance is 2.99 Å (Fig. 3c, d and e). For the higher-energy B_{1g} mode, Zr and SiO_4 vibrate out of phase, while in the lower-energy B_{1g} mode they are in phase. The total reduced mass of the latter mode is twice that of the former, which can, however, only account for approximately one half of the observed difference in their energies. The remaining half can be explained by Zr^{4+}-Si^{4+} repulsion that occurs in the out-of-phase mode but not in the in-phase one. One can estimate that the force constant of this interaction is about 0.7 of a typical divalent cation-SiO_4 interaction occurring in silicates like olivine or garnet. Such a strong repulsion is not often the case and it is a result of the high charge of the Zr cation. Fig. 3f, g and h show the three translational modes at 225 cm^{-1} (E_g), 202 cm^{-1} (E_g) and 287 cm^{-1} (E_u) occurring in the *ab* crystal plane. The reason for their difference in energy is not clear. Note that the E_u mode represents a transverse vibration where a long-range electrical field does not occur.

Mode intensities

As mentioned above, the intensities of the SiO_4 stretching vibrations are governed not only by their intrinsic polarizability, but by the electronic state of Zr^{4+}. The valence electrons of the Zr^{4+} cation are shared with surrounding oxygen atoms. Internal vibrations within the SiO_4 group modulate the electron density of the Zr^{4+}-oxygen bonds and it is reasonable to propose, therefore, that scattering related to the SiO_4 stretching vibrations will

have the greatest intensity when their symmetry is coincident with the symmetry of the Zr-O bonds. To analyze these bonds the symmetry of the Zr^{4+} electronic state, as well as the symmetry of the eight oxygen ligands in the dodecahedron, must be considered. To do this in a rigorous way would require elaborate lattice dynamic/electronic structure calculations. Instead, we will try to describe the interaction by considering simply the symmetry of the valence electrons. The electronic state of Zr^{4+} is $4d^25s^2$ and all four valence electrons take part in the bonding. The site symmetry of Zr is lowered from O_h in an undistorted dodecahedron to D_{2d} in zircon and the symmetry of the s- and d-orbitals in the D_{2d} point group and D_{4h} factor group of the crystal are as follows:

State	*s*	d_{xy}	d_{xz}	d_{yz}	$d_{x^2y^2}$	d_{z^2}
Site group D_{2d}	A_1	B_2	E	E	B_1	A_1
Factor group D_{4h}	A_{1g}	B_{2g}	E_g	E_g	B_{1g}	A_{1g}

In an ideal triangular dodecahedron the oxygen atoms surrounding Zr^{4+} are at the corners of a cube. However, there are two sets of crystallographically independent Zr-O bonds in zircon, four with a shorter distance of 2.13 Å, that are directed towards the shared edges of neighboring dodecahedra and four longer distances of length 2.27 Å that are directed to the oxygen atoms of the shared tetrahedral-dodecahedral edges (Fig. 1). The shorter bonds form an almost square planar coordination around Zr in the *aa* plane. The other set of bonds is perpendicular to them in the *ac* plane. The distortion of the triangular dodecahedron results in a strong interaction between the $d_{x^2-y^2}$ (B_{1g}) and s (A_{1g}) metal states in the Zr-O bonding. Since the d orbitals are more delocalized, their influence on the mode intensity should be greater. This can possibly explain the strong intensity of the SiO_4 stretching vibration at 1008 cm^{-1} in the B_{1g} spectrum (Fig. 2), which has the same symmetry as the $d_{x^2-y^2}$ orbitals. It can, in addition, explain why the intensity of the A_{1g} stretching motion of SiO_4 at 974 cm^{-1} is considerably greater in the *aa* spectrum than in *cc*.

The lower energy bending motions υ_2 and υ_4, the hindered rotation $R(SiO_4)$, and the $T(SiO_4)$ translation mix and interact with Zr vibrations. Their vibrational behavior is too complicated to determine here and state-of-the-art lattice dynamic calculations are required to interpret them correctly.

Comparison to garnet

All the Raman and IR modes in zircon increase slightly in wave number upon cooling from 295 K to 90 K (Dawson *et al.*, 1971; Syme *et al.*, 1977). This is not the case in pyrope garnet, $Mg_3Al_2(SiO_4)_3$, where low-energy vibrations related to the Mg cation soften slightly with decreasing temperature (Geiger *et al*., 1992; Boffa Ballaran *et al.*, 1999; Kolesov & Geiger, 2000). Thus the dodecahedral Mg cations in pyrope have a more anharmonic character than vibrations in zircon, which are notably harmonic (Syme *et al.*, 1977). This is probably related to the strong Zr-O bonding occurring in the *aa* plane of zircon. In addition, the high charge of Zr^{4+} generates repulsive interactions with Si^{4+}, which in turn causes the high wave numbers of some of the Zr-SiO_4 translational modes. In garnet, in comparison, the wave numbers of the divalent **E**-site cation and SiO_4 translations are lower in energy and are generally found between 180-280 cm^{-1}. Finally, the similarity in mass between Zr and the SiO_4 groups does not permit pure translational vibrations to be observed as in the case of garnet, where, for example, a band at 200 cm^{-1} is almost a pure $T(SiO_4)$ mode.

Acknowledgments: We thank Prof. G.R. Rossman for supplying us with the single crystals used in this study. Drs. E. Libowitzky and L. Nasdala are thanked for their careful reviews of the manuscript. This work was generously supported by a grant from the Volkswagen-Stiftung I/72 951.

References

Armbruster, T. & Geiger, C.A. (1993): Andradite crystal chemistry, dynamic X-site disorder and structural strain in silicate garnets. *Eur. J. Mineral.*, **5**, 59-71.

Boffa Ballaran, T., Carpenter, M.A., Geiger, C.A., Koziol, A. (1999): Local structural heterogeneity in garnet solid solutions. *Phys. Chem. Minerals*, **26**, 554-569.

Chase, A.B. & Osmer, J.A. (1966): Growth and preferential doping of zircon and thorite. *J. Electrochem. Soc*., **113**, 198-199.

Dawson, P., Hargreave, M.M., Wilkinson, G.R. (1971): The vibrational spectrum of zircon ($ZrSiO_4$). *J. Phys. C: Solid State Phys.*, **4**, 240-256.

Enraf Nonius (1983): Structure determination package (SDP). Enraf Nonius, Delft, Holland.

Ewing, R.C., Lutze, W., Weber, W.J. (1995): Zircon: A host-phase for the disposal of weapons plutonium. *J. Mat. Res.*, **10**, 243-246.

Finger, L.W. (1973): Structure of zircon. *Carnegie Inst. Wash. Year Book*, **72**, 544-547.

Geiger, C.A., Merwin, L., Sebald, A. (1992): Structural investigation of pyrope garnet using temperature-dependent FTIR and ^{29}Si and ^{27}Al MAS NMR spectroscopy. *Am. Mineral.*, **77**, 713-717.

Hazen, R.M. & Finger, L.W. (1979): Crystal structure and compressibility of zircon at high pressure. *Am. Mineral.*, **64**, 196-201.

Hassel, O. (1926): Die Kristallstruktur einiger Verbindungen von der Zusammensetzung MRO_4.- I. Zirkon $ZrSiO_4$. *Z. Kristall.*, **63**, 247-254.

Kieffer, S.W. (1985): Heat capacity and entropy: Systematic relations to lattice entropy. *Rev. Mineral.*, **14**, 65-126.

Kolesov, B.A. & Geiger, C.A. (1998): Raman spectra of silicate garnets. *Phys. Chem. Minerals*, **25**, 142-151.

Kolesov, B.A. & Geiger, C.A. (2000): Low-temperature single-crystal Raman spectrum of pyrope. *Phys. Chem. Minerals*, **27**, 645-649.

Krstanovic, I.R. (1958): Redetermination of the oxygen parameters in zircon ($ZrSiO_4$). *Acta Cryst.*, **11**, 896-897.

Kunz, M. & Armbruster. T. (1990): Difference displacement parameters in alkali feldspars: Effects of (Si,Al) order-disorder. *Am. Mineral.*, **75**, 141-149.

Mursic, Z., Vogt, T., Boysen, H., Frey, F. (1992a): Single-crystal neutron diffraction study of metamict zircon up to 2000 K. *J. Appl. Cryst.*, **25**, 519-523.

Mursic, Z., Vogt, T., Frey, F. (1992b): High-temperature neutron powder diffraction study of $ZrSiO_4$ up to 1900 K. *Acta Cryst.*, **B48**, 584-590.

Nicola, J.H. & Rutt, H.M. (1974): A comparative study of zircon ($ZrSiO_4$) and hafnon ($HfSiO_4$) Raman spectra. *J. Phys. C: Solid State Phys.,* **7**, 1381-1386.

Rios, S., Malcherek, T., Salje, E.K.H., Domeneghetti, C. (2000): Localized defects in radiation-damaged zircon. *Acta Cryst*., **B56**, 947-952.

Robinson, K., Gibbs, G.V., Ribbe, P.H. (1971): The structure of zircon: a comparison with garnet. *Am. Mineral.*, **56**, 782-790.

Schomaker, V. & Trueblood, K.N. (1968): On the rigid-body motion of molecules in crystals. *Acta Cryst.*, **B24**, 63-76.

Sheldrick, G.M. (1997): SHELXL-97 and SHELXS-97. Programs for crystal structure determination. University of Göttingen, Germany.

Siggel, A. & Jansen, M. (1990): Röntgenographische Untersuchungen zur Bestimmung der Einbauposition von Seltenen Erden (Pr, Tb) und Vanadium in Zirkonpigmenten. *Z. Anorg. Allg. Chemie*, **583**, 67-77.

Speer, J.A. (1980): Zircon. *Rev. Mineral.*, **5**, 67-112.

Syme, R.W.G., Lockwood, D.J., Kerr, H.J. (1977): Raman spectrum of synthetic zircon ($ZrSiO_4$) and thorite ($ThSiO_4$). *J. Phys. C: Solid State Phys.*, **10**, 1335-1348.

Zhang, M., Salje, E.K.H., Farnan, I., Graeme-Barber, A., Daniel, P., Ewing, R.C., Clark, A.M., Leroux, H. (2000): Metamictization of zircon: Raman spectroscopic study. *J. Phys. Matter.*, **12**, 1915-1925.

Received 24 November 2000
Modified version received 9 March 2001
Accepted 23 April 2001